

## Development of a Layered Hybrid Nanocomposite Material Using $\alpha,\omega$ -Bifunctionalized Polythiophenes

Jonas Delabie, Julien De Winter, Olivier Deschaume, Carmen Bartic, Pascal Gerbaux, Thierry Verbiest, and Guy Koeckelberghs\*



Cite This: <https://dx.doi.org/10.1021/acs.macromol.0c01593>



Read Online

ACCESS |



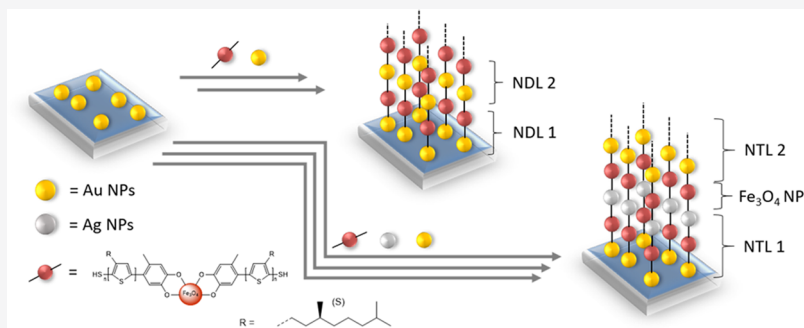
Metrics & More



Article Recommendations



Supporting Information



**ABSTRACT:** In this study, a new chiral  $\alpha,\omega$ -bifunctional polythiophene is synthesized and used as a nanoparticle linker molecule to synthesize the first layered conjugated polymer/nanoparticle (CP/NP) hybrid material to induce a potential nonreciprocal optical rotation. The bifunctionalized polythiophene (PT) is synthesized using a controlled Kumada catalyst-transfer condensation polymerization (KCTCP) mechanism utilizing a combination of a catechol-functionalized Ni-initiator and a termination process with  $S_8$  and 1,8-diazabicyclo[5.4.0]undec-7-ene (DBU), to quantitatively obtain a catechol and thiol end-capped poly(3-((S)-3,7-dimethyloctyl)thiophene). The catechol group has a high affinity for magnetite NPs, while the thiol end group prefers to bind with metallic NPs such as silver and gold. Using these properties, both a double-layered material, consisting of repeated layers of gold and magnetite NPs, and a triple layered material, consisting of gold, magnetite, and silver NPs was made, where each NP layer was linked with the previously synthesized polymer. This was achieved by first functionalizing magnetite NPs with the polymer, resulting in free thiol ends on these hybrid magnetite NPs. Using these hybrid magnetite NPs allowed for a selective layered construction by alternating a metallic layer with these hybrid magnetite NP layers. In this way, a system with up to eight double layers and a system with three triple layers was synthesized and analyzed using UV-vis and atomic force microscopy (AFM) measurements. Finally, also the nonreciprocal properties were tested.

### INTRODUCTION

Over the last 30 years conjugated polymers (CPs) have evolved from ill-defined materials into state-of-the-art macromolecules with well-defined super- and supramolecular structures, which have led to countless modern and innovative applications. This evolution, however, would have been impossible without the development of catalyst-transfer condensation polymerization (CTCP), leading to controlled chain-growth polymerization of poly(3-alkylthiophene)s (P3ATs),<sup>1–4</sup> and later also other CPs.<sup>5–10</sup> Due to the association of the transition metal catalyst with the growing polymer chain during the sequential cross-coupling reactions, chain-growth polymerization with predictable molar masses, low dispersity, and perfect control over the molecular structure and end groups is obtained. The importance of controlling the end groups in CPs cannot be underestimated as it not only has a significant impact on the supramolecular organization<sup>11,12</sup> but also allows for interesting applications like decorating

nanoparticles (NPs)<sup>13,14</sup> or making block copolymers that cannot be achieved via sequential monomer addition.<sup>15–18</sup> At first, Ni(dppp)Cl<sub>2</sub> was used as an initiator/catalyst for the controlled Kumada CTCP (KCTCP), leading to H/Br-terminated polythiophenes (PTs).<sup>2,4</sup> However, over the years new methods to implement different end functionalities on both the  $\alpha$ - and  $\omega$ -ends of CPs have been developed. In general, three different methods are commonly used. The first method relies on postpolymerization reactions to functionalize the  $\alpha$ - and/or  $\omega$ -ends. Although a wide variety of functional

Received: July 10, 2020

Revised: November 16, 2020

groups can be implemented, this method often suffers from incomplete conversions and lower yields due to the separate reaction step besides polymerization. Furthermore, post-modification sometimes requires low-temperature conditions for lithiation procedures, promoting aggregation of the CPs in the reaction medium.<sup>19</sup> The second method exploits the controlled chain-growth mechanism by adding a functionalized end-capper to terminate the polymerization.<sup>14,20,21</sup> Although this method targets the  $\omega$ -end of the polymer, it often suffers from both mono- and dicapping due to ring-walking, depending on the functional group.<sup>14,20,21</sup> The third approach makes use of functionalized Ni-initiators, often referred to as external initiators, resulting in  $\alpha$ -functionalized CPs.<sup>22–25</sup> When combined with controlled polymerization, this method gives rise to monodirectional growth with a functional group at the  $\alpha$ -end of each polymer chain. The real strength and interesting part of this method becomes obvious when combined with the termination method. As the functionalized  $\alpha$ -end inhibits the bicapping during the termination, the synthesis of CPs with two different end-group functionalities at the  $\alpha$ - and  $\omega$ -ends becomes possible.<sup>26–28</sup> Despite their interesting potential, only a limited amount of research has been dedicated toward these materials. Some examples are provided by the groups of Huck<sup>29</sup> and Bao,<sup>30</sup> who managed to use Suzuki–Miyaura CTCP to achieve both  $\alpha$ - and  $\omega$ -end functionalization, while Okamoto et al. managed to use KCTCP with an external Ni-initiator for the  $\alpha$ -end and a thiol functionality at the  $\omega$ -end by termination with sulfur powder and 1,8-diazabicyclo[5.4.0]undec-7-ene ( $S_8$ /DBU) to make the bifunctionalized poly(3-hexylthiophene).<sup>31</sup>

Recently, the group of Verbiest reported a nanocomposite system composed of a layered structure of silver, iron oxide, and gold nanoparticles attached to a glass substrate.<sup>32,33</sup> These unique materials were found to display a wide variety of unique properties ranging from nonreciprocal optical transmission<sup>33</sup> and Faraday rotation<sup>32,34</sup> to the possibility of differentiating chiral enantiomers using light carrying orbital angular momentum, which was previously considered impossible.<sup>35</sup> It was found that many of these properties originate from the strong electric-quadrupole interactions between the gold and silver nanoparticles, while the iron oxide functions as a refractive index enhancer. Although the application potential for such a material is huge, ranging from optical isolators<sup>36–38</sup> and all-optical computing and processing devices<sup>39,40</sup> to building blocks for integrated photonic circuits,<sup>41</sup> the currently observed effects are too small to make this economically viable. CPs, however, are known to demonstrate a large quadrupole behavior.<sup>42</sup> Thus, replacing the currently used inactive linker molecule by a new quadrupole active CP could enhance these well-desired nonreciprocal effects, increasing the economic viability. That is why this article aims to develop a new chiral  $\alpha,\omega$ -bifunctional polythiophene as a nanoparticle linker molecule to synthesize the first layered conjugated polymer/nanoparticle (NP) hybrid material with the goal to enhance the nonreciprocal optical rotation.

## RESULTS AND DISCUSSION

To make the layered nanocomposite material, we use a conjugated polymer with two different end groups that can bind selectively with either metallic silver and gold NPs on one end and magnetite NPs on the other end. With this in mind, poly(3-((*S*)-3,7-dimethyloctyl)thiophene) with a 4-methylcatechol at the  $\alpha$ -end and a thiol functionality on the  $\omega$ -end

was synthesized. While the catechol was chosen for its high affinity for the magnetite nanoparticles, it is also easily introduced as a functionalized nickel initiator while still leading to controlled polymerization.<sup>43</sup> At the  $\omega$ -end a thiol end group was chosen for its high affinity for both the silver and gold NPs, and can be introduced by terminating the polymerization with  $S_8$ /DBU as described by Okamoto et al.<sup>31</sup> Using two different end groups with different affinities for the NPs, a well-defined layered structure can be achieved as shown in Figure 1. Note that a chiral sidechain was used with the goal of achieving a chiral expression in the final layered material.

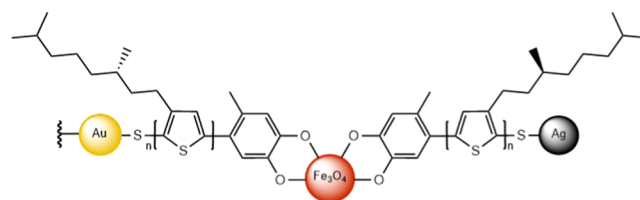


**Figure 1.** Schematic Representation of Gold, Magnetite, and Silver NPs Connected by Poly(3-((*S*)-3,7-dimethyloctyl)thiophene) with Catechol and Thiol End Groups.

**Synthesis of Polymers.** All polymers were made via a KCTCP mechanism utilizing a 4-methylcatechol functionalized Ni(dppp) initiator. Note that the hydroxyl functionalities had to be protected with an acetyl group as these would otherwise quench the active monomers during polymerization. An overview of the polymerization procedure is depicted in Scheme 1. First, the precursor monomer (*S*)-2-bromo-5-iodo-3-(3,7-dimethyloctyl)thiophene had to be converted into the active monomer (*S*)-5-magnesiocloro-2-bromo-3-(3,7-dimethyloctyl)thiophene using *i*-PrMgCl–LiCl. Meanwhile, to obtain controlled polymerization, a ligand exchange on the catalyst is performed using 2 equiv of 1,3-bis-(diphenylphosphino)-propane (dppp).<sup>44</sup> Due to the controlled nature, the degree of polymerization (DP) can be tuned by varying the  $[M_0]/[In]$  ratio, which was set to obtain a DP of 20. This will be long enough to provide sufficient quadrupole contributions from the polymer while keeping the distance between the gold and silver NPs fairly small. After addition of the monomer to the controlled initiator species, the reaction mixture was stirred for 1 h before it was split into two separate batches. One batch was terminated with a 2M HCl solution in tetrahydrofuran (THF), resulting in H-terminated polymers (P1), while the second batch was added to a solution of  $S_8$ /DBU and stirred for 30 min before it was quenched with the same HCl solution, resulting in thiol-terminated polymers (P2).

Table 1 lists the molar mass and polydispersity, determined via gel permeation chromatography (GPC) toward polystyrene standards, and the DP, determined with <sup>1</sup>H NMR. It is important to note that GPC tends to overestimate the molar mass of polythiophenes due to their more rigid backbone compared to the polystyrene standards.<sup>43,45</sup> Low dispersity values were obtained, as to be expected from a controlled synthesis. Although both polymers arise from the same polymerization, a difference in molar mass and a shift in GPC is observed (Supporting Information Figure S1). This, however, can be explained by the formation of thiol-bridges between the thiol-terminated polymers (P2), resulting in polymer fractions with a double molar mass, which increases

## Scheme 1. Synthesis of Polymers P1 and P2

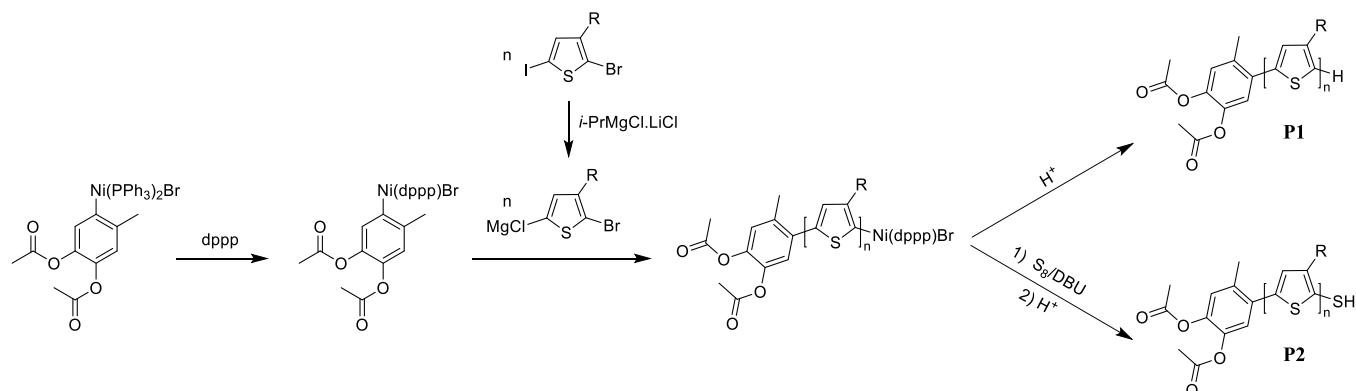


**Table 1.**  $M_n$ , Dispersity, and the Degree of Polymerization for P1 and P2

polymer	$M_n$ (kg·mol <sup>-1</sup> )	peak $M_n$ (kg·mol <sup>-1</sup> )	$D_M$	DP
P1	6.1	7.4	1.1	22
P2	10.3	13.8	1.2	22

the number average molar mass and results in a slightly higher molar mass dispersity. This becomes especially obvious when comparing the peak molar masses of both polymers, which is twice as big for P2. The DP was found to be 22 for both polymers, which is close to the aimed DP of 20. Note that NMR does not give rise to a double molar mass even when S–S bridges are formed because calibration was performed on the 4-methylene group of the catechol, which is present at both ends of the S–S bridged polymer chains.

To determine the success of the end-capping, <sup>1</sup>H NMR was used in combination with MALDI-ToF. Figure 2 shows how in particular the signal for the terminal  $\alpha$ -methylene protons (2.62 ppm, e) of P1 shifts underneath the signal for the internal  $\alpha$ -methylene protons (2.80 ppm, d) for P2, caused by the end-capped thiol functionality. Furthermore, two distinct singlets can be observed at 2.46 ppm (a) and 2.37 ppm (b), originating from the 4-methylene protons of both protected

and deprotected 4-methyl-catechol, respectively. Because the desired DP was obtained, meaning no monomer was destroyed, the deprotection probably takes place upon termination of polymerization with acid, which is a well-known acetyl deprotection protocol. This, however, poses no problem as the hydroxyl groups have to be deprotected eventually before they can be used for functionalization of the magnetite NPs. Finally, the doublet at 2.30 ppm (c) originates from acetyl groups and is always twice the integration of singlet a due to the two protected hydroxyl groups. To get additional information on the nature of the end groups, mass spectrometry analyses have been performed (Figures S4 and S5). As expected, P1 is mainly characterized by the polythiophene with protected catechol as the  $\alpha$ -moiety and hydrogen as the  $\omega$ -end group. The main distribution of P2 is shifted to a higher mass to charge ratio corresponding to the 31 mass unit. However, the expected mass difference between P1 and P2 is 32 mass units (addition of a sulfur atom), and this mass difference probably corresponds to the loss of one hydrogen atom ( $H^0$ ) during the ionization process as attested by the comparison between the experimental and the theoretical isotopic models. Both mass analyses confirm the successful synthesis.

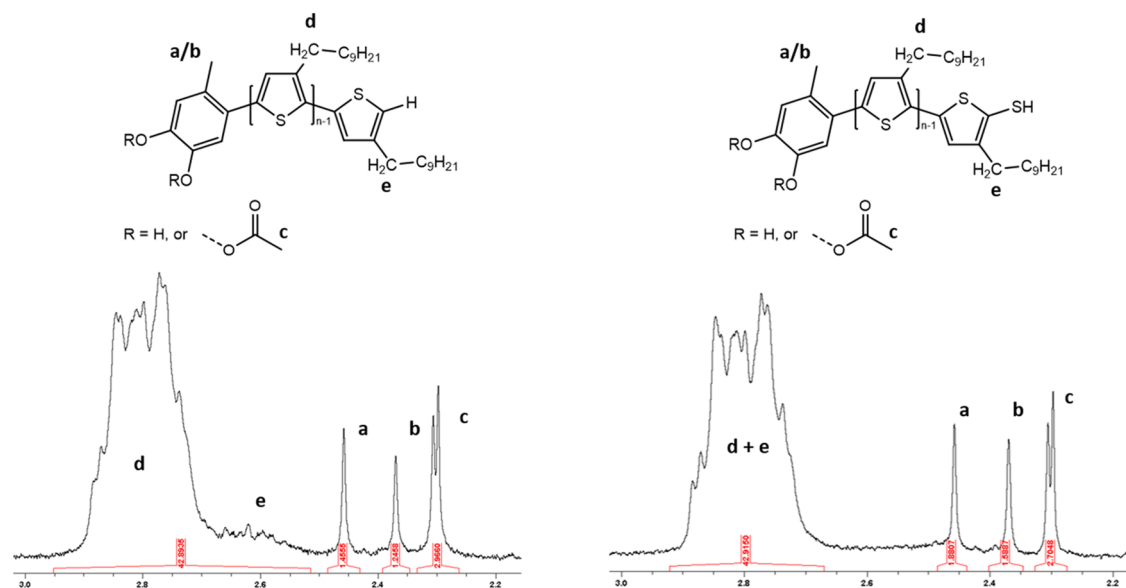


**Figure 2.** Overview of <sup>1</sup>H NMR spectra of P1 and P2.

**Synthesis and Analysis of Hybrid Magnetite NPs.** Oleic acid-stabilized magnetite NPs of  $10 \pm 3$  nm were used for the functionalization (see the Supporting Information). However, to functionalize these NPs with P2, the remaining acetyl groups first need to be removed. This was done *in situ* by dispersing the magnetite NPs and P2 in THF and adding a small amount of ammonia solution. This deprotects the hydroxyl groups of the catechol, making them available for ligand exchange with the oleic acid chains on the magnetite NPs. This exchange is entropically favored by the bidentate nature of catechol, making this exchange fairly easy. Note how also small amounts of the reducing agent (dithiothreitol, DTT) were added to break up potential disulfide bonds and prevent the formation of both polymer and magnetite NP aggregates. The solution was stirred for 2 h, followed by precipitation of the NPs and the remaining free polymer in MeOH. Due to their superparamagnetic nature, the hybrid magnetite NPs could be separated from the free polymer via magnetic separation. To ensure that no free polymer remains, the hybrid NPs were dispersed in THF, which is a good solvent for both the polymer and the NPs, and purified via magnetic separation. While the polymer remains in solution, the NPs will precipitate in the presence of a strong magnet. These purified NPs are then dried, weighed, dispersed in THF to a concentration of  $3 \text{ mg mL}^{-1}$ , and subsequently analyzed by UV-vis spectrometry. Figure 3 shows the UV-vis spectra of the magnetite NPs

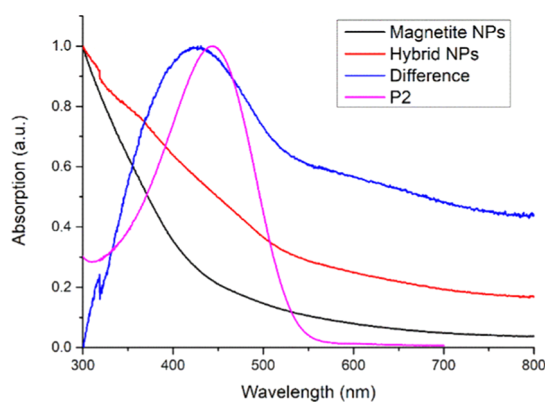


**Figure 3.** Normalized UV-vis spectra of oleic acid-stabilized NPs (black), hybrid P2/magnetite NPs (red), and the difference between the hybrid and oleic acid-stabilized NPs (blue) compared to the pure polymer P2 (purple).

before and after functionalization with P2. At the first glance there seems to be no clear indication of the presence of the polymer. However, when subtracting the spectra of the hybrid NPs with the original NPs a UV-vis spectrum is obtained that is in very good correspondence with the UV-vis spectrum of the pure polymer, indicating the successful synthesis of the hybrid magnetite material. Transmission electron microscopy (TEM) measurements show no further noteworthy degradation or loss of the quality of the nanoparticles (Figures S8 and S9).

**Synthesis and Analysis of the Layered Nanocomposite Materials. Double-Layered Nanocomposite Materials.** The first layered nanocomposite system was made by coating a glass substrate with (3-aminopropyl)trimethoxysilane (APTMS), on which the gold NPs ( $11 \pm 1$  nm) were deposited. Next, the hybrid magnetite NPs, equipped with the free thiol groups of P2, were deposited on top of the gold NPs, leading to a nanoparticle double layer (NDL) connected by a conjugated polymer. The deposition of these NDLs was repeated up to eight times and UV-vis measurements were made after each NDL deposition (Figure 4). These UV-vis spectra display a nice increase in absorption with each DL, proving successful nanoparticle deposition. Note, however, the larger increase of absorption around 350 nm, originating from the hybrid magnetite NPs, compared to the signal around 550 nm, originating from the gold NPs. A possible explanation could be that magnetite has a larger molar attenuation coefficient than gold. However, the most likely explanation is found by looking at the atomic force microscopy (AFM) measurements. Although an overall increase of thickness is observed with each NDL deposition, there is also a visible aggregate formation most likely from the magnetite NPs (Figures S10 and S11), leading to increased absorption compared to the gold NPs. The average thickness of 7 DL was found to be 110 nm, which is almost twice the thickness of the previously made material by Brullot et al. with 7 DL.<sup>32</sup> This makes sense as now a much longer polymer chain is used as a linker molecule between the NPs, compared to the short aminosiloxane linker used in previous systems. The presence of gold and iron was also confirmed by total reflection X-ray fluorescence (TXRF) analysis (Figure S14).

**Triple Layered Nanocomposite Material.** A second nanocomposite material was made consisting of layers of gold, hybrid magnetite, and silver NPs forming nanoparticle triple layers (NTLs). This system was made in a way similar to that

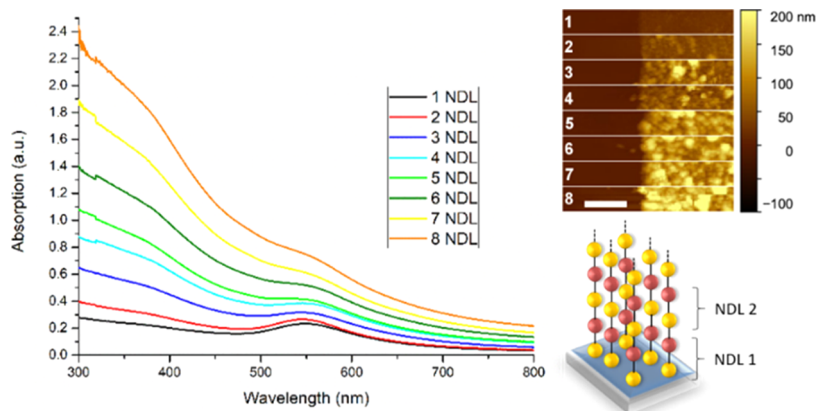


**Figure 4.** UV-vis (left) and AFM (right) measurements of each double layer consisting of gold and hybrid magnetite NPs, respectively.

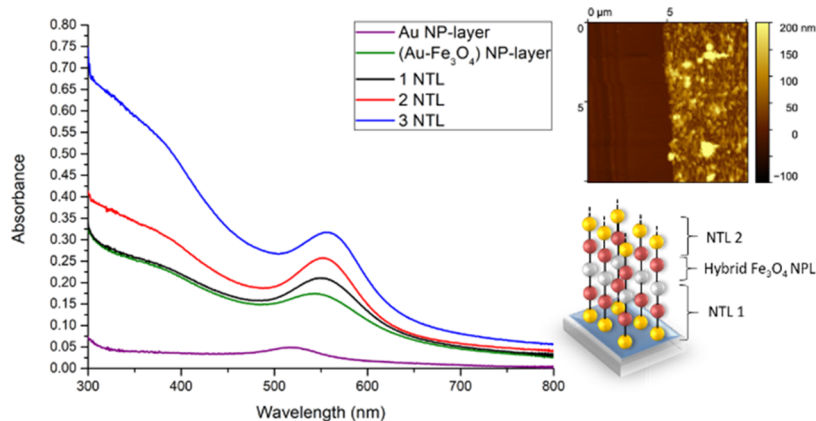


Figure 5. UV-vis of each triple layer consisting of gold, hybrid magnetite, and silver NPs, respectively.

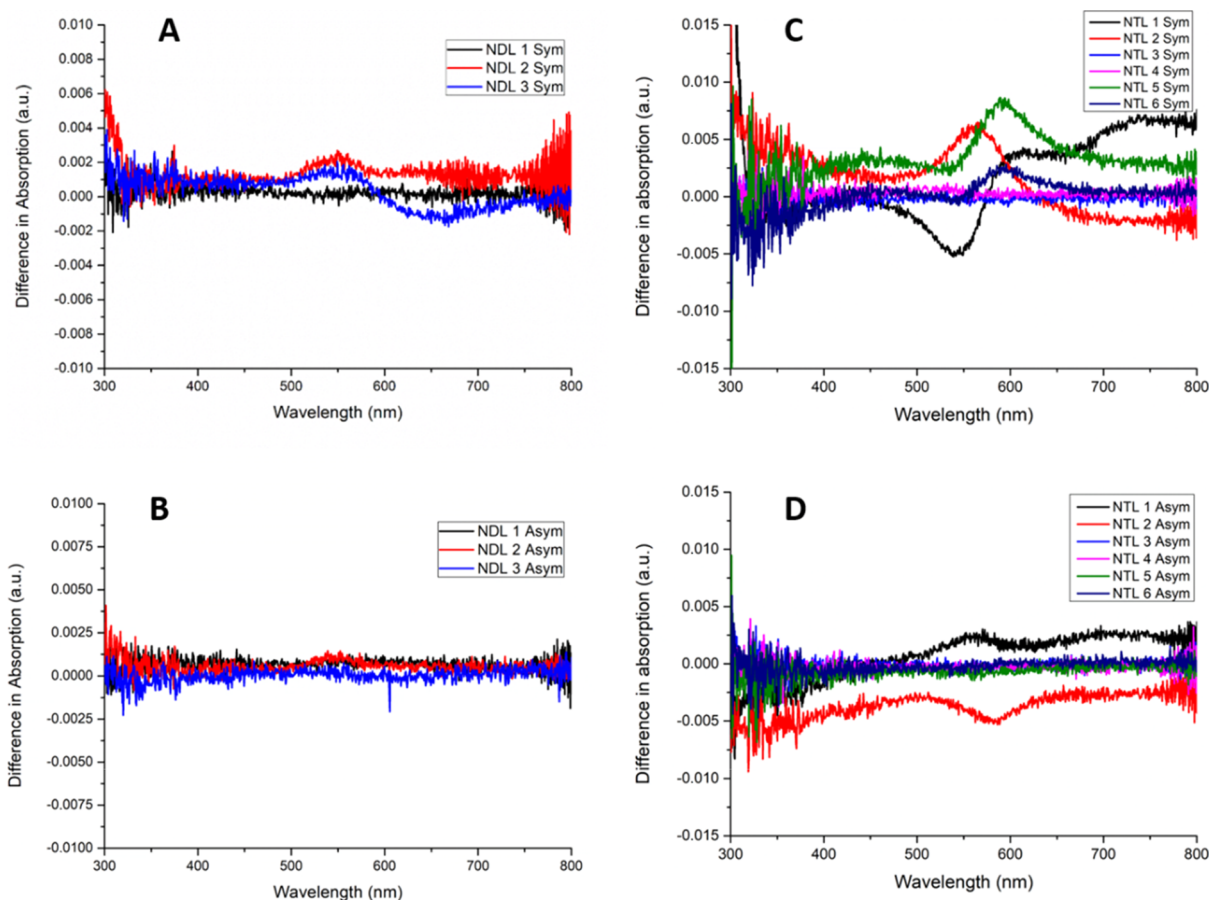


Figure 6. Difference in absorption between the front and backsides of the symmetric and asymmetric NDL (A and B) and NTL (C and D) nanocomposite structures.

of the NDL material, except that after the first hybrid magnetite NP layer a silver NP layer was deposited on top, creating the NTL. A nanocomposite structure was made with up to three NTLs. It is important to note that in between each NTL, a hybrid magnetite NP layer was added to connect the silver NPs of the NTL with the gold NP layer of the next NTL, resulting in a total of 11 NP layers, similar to the 16 NP layers of the double-layered material. UV-vis was measured again after each NTL and clearly shows an increased absorption after each NTL (Figure 5). Additionally, the presence of the gold and iron oxide NPs was confirmed by TXRF measurements (Figure S15). Unfortunately, the silver NPs did not dissolve in

the aqua regia used for the sample preparation due to the formation of AgCl. Furthermore, this is combined with an overlap on TXRF between the  $L\alpha$  lines from silver with the  $K\alpha$  lines from argon, making the detection of Ag NPs using TXRF impossible. Nevertheless, UV-vis clearly shows a difference after deposition of the Ag NPs on top of the Au- $\text{Fe}_3\text{O}_4$ -layered material and the material is both visually and on UV-vis different from the NDL material, demonstrating a successful synthesis of the NTL nanocomposite material.

**Analysis of Nonreciprocal Properties.** Both the NDL and NTL composite systems were analyzed for their nonreciprocal properties using UV-vis spectrometry. Due to

the nature of the nanocomposite synthesis, both sides of the glass substrate were covered, resulting in a symmetric material. However, because nonreciprocity only manifests in asymmetric materials,<sup>39</sup> one side of the glass substrate was removed using a tissue soaked in MeOH. First, UV–vis measurements were taken from the front and back sides of the symmetrical system, where the nonreciprocity should be absent. Next the nanoparticle layers on one side were removed and the front and backside of the sample were measured once more. Figure 6 shows an overview of the difference in absorption between the back and the front side for both the symmetric and asymmetric materials performed on different samples.

When looking at the differences in the symmetric materials, it immediately stands out that the difference in absorption is not always zero. Because nonreciprocity is highly unlikely in symmetric materials, this difference is probably due to irregularities of the sample. Furthermore, when comparing the symmetric and asymmetric materials, when a difference in absorption is observed for the symmetric sample, there is often also a difference for the asymmetric sample. On the other hand, when there is no difference in absorption for the symmetric sample, indicating a more homogeneous sample, there is also no difference observed for the asymmetric material. This leads us to conclude that there is no significant nonreciprocal effect present in the nanocomposite material for both the NDL and NTL systems.

There could be several reasons for the absence of nonreciprocity. First of all, using a polymer automatically introduces a dispersity in the layered material, which could lead to a disruption of the quadrupole interactions instead of enhancing them. Even though the dispersity of the synthesized polymer was rather small, there is still a large difference compared to a well-defined small organic molecule. Furthermore, it is possible that by linking the metallic NPs with a CP, the NPs are too far apart to induce a quadrupole moment, which could not be compensated by the CP's own quadrupole contributions.<sup>33</sup> Finally, from the absence of a chiral response of the layered hybrid materials (Figures S18 and S19), it can be concluded that intramolecular stacking and thereby also the quadrupole contribution of the polythiophenes are inhibited.<sup>42,43</sup>

## CONCLUSIONS

In conclusion, we have succeeded in the synthesis of a new, tailor-made  $\alpha,\omega$ -bifunctionalized poly(3-(S-3,7-dimethyloctyl)-thiophene) with two different end groups. A high degree of selective end-capping was obtained using a catechol-functionalized external Ni-initiator to obtain a catechol end group at the  $\alpha$ -end, while the  $\omega$ -end was functionalized via termination with  $S_8$ /DBU to obtain a thiol-functionalized polymer. Because of the high affinity of the catechol groups for magnetite NPs, this polymer was successfully used for the coating of magnetite NPs, resulting in polymer hybrid magnetite NPs bearing free thiol end groups. Finally, these hybrid nanoparticles were used for the development of the first ever CP/NP-layered hybrid material consisting of either alternating gold and hybrid magnetite NPs (NDL system) or alternating layers of, gold, hybrid magnetite, and silver NPs (NTL system). Although the material showed signs of magnetite NP aggregation, a significant amount of layers could be constructed resulting in a unique material where each nanoparticle layer was connected via an  $\alpha,\omega$ -bifunctionalized conjugated polymer. Nevertheless, due to the inherent polydispersity of the CPs, it was impossible

to obtain a smooth sample, which in turn disrupted the nonreciprocal effect instead of enhancing it. This could potentially be solved by synthesizing conjugated oligomers step by step. However, this would significantly increase the production cost and thus make the system less economically interesting.

## ASSOCIATED CONTENT

### Supporting Information

The Supporting Information is available free of charge at <https://pubs.acs.org/doi/10.1021/acs.macromol.0c01593>.

Additional information about the materials and methods; <sup>1</sup>H NMR spectra; GPC spectra; MALDI-TOF analysis; TEM images of the nanoparticle materials; AFM-measurements of the layered nanoparticle materials; UV–vis spectra from the nonreciprocal measurements; and CD-spectra of the layered nanoparticle materials (PDF)

## AUTHOR INFORMATION

### Corresponding Author

Guy Koeckelberghs – Laboratory for Polymer Synthesis, KU Leuven, B-3001 Heverlee, Belgium; [orcid.org/0000-0003-1412-8454](https://orcid.org/0000-0003-1412-8454); Email: [guy.koeckelberghs@kuleuven.be](mailto:guy.koeckelberghs@kuleuven.be)

### Authors

Jonas Delabie – Laboratory for Polymer Synthesis, KU Leuven, B-3001 Heverlee, Belgium

Julien De Winter – Organic Synthesis and Mass Spectrometry Laboratory, Research Institute for Materials Science and Engineering, University of Mons/UMONS, B-7000 Mons, Belgium; [orcid.org/0000-0003-3429-5911](https://orcid.org/0000-0003-3429-5911)

Olivier Deschaume – Laboratory for Soft Matter and Biophysics, KU Leuven, B-3001 Heverlee, Belgium; [orcid.org/0000-0001-6222-0947](https://orcid.org/0000-0001-6222-0947)

Carmen Bartic – Laboratory for Soft Matter and Biophysics, KU Leuven, B-3001 Heverlee, Belgium; [orcid.org/0000-0001-9577-2844](https://orcid.org/0000-0001-9577-2844)

Pascal Gerboux – Organic Synthesis and Mass Spectrometry Laboratory, Research Institute for Materials Science and Engineering, University of Mons/UMONS, B-7000 Mons, Belgium; [orcid.org/0000-0001-5114-4352](https://orcid.org/0000-0001-5114-4352)

Thierry Verbiest – Laboratory for Molecular Electronics and Photonics, KU Leuven, B-3001 Heverlee, Belgium

Complete contact information is available at:

<https://pubs.acs.org/doi/10.1021/acs.macromol.0c01593>

### Author Contributions

The manuscript was written through contributions of all authors. All authors have given approval to the final version of the manuscript.

### Notes

The authors declare no competing financial interest.

## ACKNOWLEDGMENTS

This research was funded by the Fund for Scientific Research (FWO Flanders—1S04317N) and the Research Fund KU Leuven. J.D. is funded by FWO-SB. Arne Billen is acknowledged for the synthesis of the magnetite NPs and Maarten Eerdeken is acknowledged for performing TEM measurements. The UMONS MS lab is grateful to the “Fonds National de la Recherche Scientifique (FRS-FNRS)” for financial

support for the acquisition of the Waters QToF Premier mass spectrometer. O.D. and C.B. acknowledge the funding by FWO Flanders (G0947.17N) and KU Leuven BOF grants C14/18/061 and C14/16/063.

## REFERENCES

- (1) Yokoyama, A.; Miyakoshi, R.; Yokozawa, T. Chain-Growth Polymerization for Poly(3-Hexylthiophene) with a Defined Molecular Weight and a Low Polydispersity. *Macromolecules* **2004**, *37*, 1169–1171.
- (2) Miyakoshi, R.; Yokoyama, A.; Yokozawa, T. Catalyst-Transfer Polycondensation. Mechanism of Ni-Catalyzed Chain-Growth Polymerization Leading to Well-Defined Poly(3-Hexylthiophene). *J. Am. Chem. Soc.* **2005**, *127*, 17542–17547.
- (3) Sheina, E. E.; Liu, J.; Lovu, M. C.; Laird, D. W.; McCullough, R. D. Chain Growth Mechanism for Regioregular Nickel-Initiated Cross-Coupling Polymerizations. *Macromolecules* **2004**, *37*, 3526–3528.
- (4) Iovu, M. C.; Sheina, E. E.; Gil, R. R.; McCullough, R. D. Experimental Evidence for the Quasi-“Living” Nature of the Grignard Metathesis Method for the Synthesis of Regioregular Poly(3-Alkylthiophenes). *Macromolecules* **2005**, *38*, 8649–8656.
- (5) Wu, S.; Sun, Y.; Huang, L.; Wang, J.; Zhou, Y.; Geng, Y.; Wang, F. Grignard Metathesis Chain-Growth Polymerization for Poly-(Bithienylmethylene)s: Ni Catalyst Can Transfer across the Non-conjugated Monomer. *Macromolecules* **2010**, *43*, 4438–4440.
- (6) Stefan, M. C.; Javier, A. E.; Osaka, I.; McCullough, R. D. Grignard Metathesis Method (GRIM): Toward a Universal Method for the Synthesis of Conjugated Polymers. *Macromolecules* **2009**, *42*, 30–32.
- (7) Nanashima, Y.; Yokoyama, A.; Yokozawa, T. Synthesis of Well-Defined Poly(2-Alkoxy-pyridine-3,5-Diyl) via Ni-Catalyst-Transfer Condensation Polymerization. *Macromolecules* **2012**, *45*, 2609–2613.
- (8) Yokoyama, A.; Kato, A.; Miyakoshi, R.; Yokozawa, T. Precision Synthesis of Poly(N-Hexylpyrrole) and Its Diblock Copolymer with Poly(p-Phenylene) via Catalyst-Transfer Polycondensation. *Macromolecules* **2008**, *41*, 7271–7273.
- (9) Miyakoshi, R.; Shimono, K.; Yokoyama, A.; Yokozawa, T. Catalyst-Transfer Polycondensation for the Synthesis of Poly(p-Phenylene) with Controlled Molecular Weight and Low Polydispersity. *J. Am. Chem. Soc.* **2006**, *128*, 16012–16013.
- (10) Sui, A.; Shi, X.; Wu, S.; Tian, H.; Geng, Y.; Wang, F. Controlled Synthesis of Polyfluorenes via Kumada Catalyst Transfer Polycondensation with Ni(Acac)<sub>2</sub>/Dppp as the Catalyst. *Macromolecules* **2012**, *45*, 5436–5443.
- (11) Van Den Eede, M. P.; Bedi, A.; Delabie, J.; De Winter, J.; Gerbaux, P.; Koeckelberghs, G. The Influence of the End-Group on the Chiral Self-Assembly of All-Conjugated Block Copolymers. *Polym. Chem.* **2017**, *8*, 5666–5672.
- (12) Koldemir, U.; Puniredd, S. R.; Wagner, M.; Tongay, S.; McCarley, T. D.; Kamenov, G. D.; Müllen, K.; Pisula, W.; Reynolds, J. R. End Capping Does Matter: Enhanced Order and Charge Transport in Conjugated Donor-Acceptor Polymers. *Macromolecules* **2015**, *48*, 6369–6377.
- (13) Monnaie, F.; Brulot, W.; Verbiest, T.; De Winter, J.; Gerbaux, P.; Smeets, A.; Koeckelberghs, G. Synthesis of End-Group Functionalized P3HT: General Protocol for P3HT/Nanoparticle Hybrids. *Macromolecules* **2013**, *46*, 8500–8508.
- (14) Kochemba, W. M.; Pickel, D. L.; Sumpter, B. G.; Chen, J.; Kilbey, S. M. In Situ Formation of Pyridyl-Functionalized Poly(3-Hexylthiophene)s via Quenching of the Grignard Metathesis Polymerization: Toward Ligands for Semiconductor Quantum Dots. *Chem. Mater.* **2012**, *24*, 4459–4467.
- (15) Ku, S. Y.; Brady, M. A.; Treat, N. D.; Cochran, J. E.; Robb, M. J.; Kramer, E. J.; Chabincyn, M. L.; Hawker, C. J. A Modular Strategy for Fully Conjugated Donor-Acceptor Block Copolymers. *J. Am. Chem. Soc.* **2012**, *134*, 16040–16046.
- (16) Lee, Y.; Aplan, M. P.; Seibers, Z. D.; Kilbey, S. M.; Wang, Q.; Gomez, E. D. Tuning the Synthesis of Fully Conjugated Block Copolymers to Minimize Architectural Heterogeneity. *J. Mater. Chem. A* **2017**, *5*, 20412–20421.
- (17) Urien, M.; Erothu, H.; Cloutet, E.; Hiorns, R. C.; Vignau, L.; Cramail, H. Poly(3-Hexylthiophene) Based Block Copolymers Prepared by “Click” Chemistry. *Macromolecules* **2008**, *41*, 7033–7040.
- (18) Van Den Bergh, K.; Willot, P.; Cornelis, D.; Verbiest, T.; Koeckelberghs, G. Influence of the Presence and Length of an Alkyl Spacer on the Supramolecular Chirality of Block Copoly(Thiophene)-S. *Macromolecules* **2011**, *44*, 728–735.
- (19) Zhang, L.; Hashimoto, K.; Tajima, K. End-Group Stannylation of Regioregular Poly(3-Hexylthiophene)S. *Polym. J.* **2012**, *44*, 1145–1148.
- (20) Jeffries-El, M.; Sauvé, G.; McCullough, R. D. Facile Synthesis of End-Functionalized Regioregular Poly(3-Alkylthiophene)s via Modified Grignard Metathesis Reaction. *Macromolecules* **2005**, *38*, 10346–10352.
- (21) Jeffries-EL, M.; Sauvé, G.; McCullough, R. D. In-Situ End-Group Functionalization of Regioregular Poly(3-Alkylthiophene) Using the Grignard Metathesis Polymerization Method. *Adv. Mater.* **2004**, *16*, 1017–1019.
- (22) Smeets, A.; Van Den Bergh, K.; De Winter, J.; Gerbaux, P.; Verbiest, T.; Koeckelberghs, G. Incorporation of Different End Groups in Conjugated Polymers Using Functional Nickel Initiators. *Macromolecules* **2009**, *42*, 7638–7641.
- (23) Smeets, A.; Willot, P.; De Winter, J.; Gerbaux, P.; Verbiest, T.; Koeckelberghs, G. End Group-Functionalization and Synthesis of Block-Copolythiophenes by Modified Nickel Initiators. *Macromolecules* **2011**, *44*, 6017–6025.
- (24) Bronstein, H. A.; Luscombe, C. K. Externally Initiated Regioregular P3HT with Controlled Molecular Weight and Narrow Polydispersity. *J. Am. Chem. Soc.* **2009**, *131*, 12894–12895.
- (25) Yokoyama, A.; Suzuki, H.; Kubota, Y.; Ohuchi, K.; Higashimura, H.; Yokozawa, T. Chain-Growth Polymerization for the Synthesis of Polyfluorene via Suzuki Miyaura Coupling Reaction from an Externally Added Initiator Unit. *J. Am. Chem. Soc.* **2007**, *129*, 7236–7237.
- (26) Lohwasser, R. H.; Bandara, J.; Thelakkat, M. Tailor-Made Synthesis of Poly(3-Hexylthiophene) with Carboxylic End Groups and Its Application as a Polymer Sensitizer in Solid-State Dye-Sensitized Solar Cells. *J. Mater. Chem.* **2009**, *19*, 4126–4130.
- (27) Langeveld-Voss, B. M. W.; Janssen, R. A. J.; Spiering, A. J. H.; Van Dongen, J. L. J.; Vonk, E. C.; Claessens, H. A. End-Group Modification of Regioregular Poly(3-Alkylthiophene)S. *Chem. Commun.* **2000**, 81–82.
- (28) Krüger, R. A.; Gordon, T. J.; Baumgartner, T.; Sutherland, T. C. End-Group Functionalization of Poly(3-Hexylthiophene) as an Efficient Route to Photosensitize Nanocrystalline TiO<sub>2</sub> Films for Photovoltaic Applications. *ACS Appl. Mater. Interfaces* **2011**, *3*, 2031–2041.
- (29) Elmalem, E.; Biedermann, F.; Johnson, K.; Friend, R. H.; Huck, W. T. S. Synthesis and Photophysics of Fully  $\pi$ -Conjugated Heterobis-Functionalized Polymeric Molecular Wires via Suzuki Chain-Growth Polymerization. *J. Am. Chem. Soc.* **2012**, *134*, 17769–17777.
- (30) Lee, J. K.; Ko, S.; Bao, Z. In Situ Hetero End-Functionalized Polythiophene and Subsequent “Click” Chemistry with DNA. *Macromol. Rapid Commun.* **2012**, *33*, 938–942.
- (31) Okamoto, K.; Luscombe, C. K. Simple Procedure for Mono- and Bis-End-Functionalization of Regioregular Poly(3-Hexylthiophene)s Using Chalcogens. *Chem. Commun.* **2014**, *50*, 5310–5312.
- (32) Brulot, W.; Strobbe, R.; Bynens, M.; Bloemen, M.; Demeyer, P. J.; Vanderlinden, W.; De Feyter, S.; Valev, V. K.; Verbiest, T. Layer-by-Layer Synthesis and Tunable Optical Properties of Hybrid Magnetic-Plasmonic Nanocomposites Using Short Bifunctional Molecular Linkers. *Mater. Lett.* **2014**, *118*, 99–102.
- (33) Brulot, W.; Swusten, T.; Verbiest, T. Broadband Nonreciprocal Quadrupolarization-Induced Asymmetric Transmission (Q-AT) in

Plasmonic Nanoparticle Aggregates. *Adv. Mater.* **2015**, *27*, 2485–2488.

(34) Stryckers, J.; Swusten, T.; Brullot, W.; D'Haen, J.; Verbiest, T.; Deferme, W. Ultrasonic Spray Coating as a Fast Alternative Technique for the Deposition of Hybrid Magnetic-Plasmonic Nanocomposites. *Adv. Eng. Mater.* **2018**, *20*, No. 1800681.

(35) Brullot, W.; Vanbel, M. K.; Swusten, T.; Verbiest, T. Resolving Enantiomers Using the Optical Angular Momentum of Twisted Light. *Sci. Adv.* **2016**, *2*, No. e1501349.

(36) Fan, L.; Wang, J.; Varghese, L. T.; Shen, H.; Niu, B.; Xuan, Y.; Weiner, A. M.; Qi, M. An All-Silicon Passive Optical Diode. *Science* **2012**, *335*, 447–450.

(37) Jalas, D.; Petrov, A.; Eich, M.; Freude, W.; Fan, S.; Yu, Z.; Baets, R.; Popović, M.; Melloni, A.; Joannopoulos, J. D.; Vanwolleghem, M.; Doerr, C. R.; Renner, H. What Is — and What Is Not — an Optical Isolator. *Nat. Photonics* **2013**, *7*, 579–582.

(38) Chin, J. Y.; Steinle, T.; Wehlius, T.; Dregely, D.; Weiss, T.; Belotelov, V. I.; Stritzker, B.; Giessen, H. Nonreciprocal Plasmonics Enables Giant Enhancement of Thin-Film Faraday Rotation. *Nat. Commun.* **2013**, *4*, No. 1599.

(39) Xu, J.; Zhuang, X.; Guo, P.; Huang, W.; Hu, W.; Zhang, Q.; Wan, Q.; Zhu, X.; Yang, Z.; Tong, L.; Duan, X.; Pan, A. Asymmetric Light Propagation in Composition-Graded Semiconductor Nanowires. *Sci. Rep.* **2012**, *2*, No. 184301.

(40) Lenferink, E. J.; Wei, G.; Stern, N. P. Coherent Optical Non-Reciprocity in Axisymmetric Resonators. *Opt. Express* **2014**, *22*, 16099.

(41) Aroua, W.; Abdelmalek, F.; Haxha, S.; Tesfa, S.; Bouchriha, H. Mode Converter Optical Isolator Based on Dual Negative Refraction Photonic Crystal. *IEEE J. Quantum Electron.* **2014**, *50*, 633–638.

(42) Verbiest, T.; Sioncke, S.; Koeckelberghs, G.; Samyn, C.; Persoons, A.; Botek, E.; André, J.; Champagne, B. Nonlinear Optical Properties of Spincoated Films of Chiral Polythiophenes. *Chem. Phys. Lett.* **2005**, *404*, 112–115.

(43) Ceunen, W.; Van Oosten, A.; Vleugels, R.; De Winter, J.; Gerbaux, P.; Li, Z.; De Feyter, S.; Verbiest, T.; Koeckelberghs, G. Synthesis and Supramolecular Organization of Chiral Poly-(Thiophene)-Magnetite Hybrid Nanoparticles. *Polym. Chem.* **2018**, *9*, 3029–3036.

(44) Smeets, A.; Van Den Bergh, K.; De Winter, J.; Gerbaux, P.; Verbiest, T.; Koeckelberghs, G. Incorporation of Different End Groups in Conjugated Polymers Using Functional Nickel Initiators. *Macromolecules* **2009**, *42*, 7638–7641.

(45) Winter, J.; De Deshayes, G.; Boon, F.; Coulembier, O.; Dubois, P.; Gerbaux, P. MALDI-ToF Analysis of Polythiophene: Use of Trans-2-[3-(4-t-Butyl-Phenyl)-2-Methyl-2-Propenylidene]-Malononitrile-DCTB-as Matrix. *J. Mass Spectrom.* **2011**, *46*, 237–246.